Temporal rainfall disaggregation with a cascade model: from single-station disaggregation to spatial rainfall

H. Müller[1] and U. Haberlandt[2]

[1]Graduate Student, Institute of Water Resources Management, Hydrology and Agricultural Hydraulic Engineering, Leibniz Universität Hannover, Appelstraße 9a, 30167 Hannover, E-Mail: mueller@iww.uni-hannover.de

[2]Professor, Institute of Water Resources Management, Hydrology and Agricultural Hydraulic Engineering, Leibniz Universität Hannover, Appelstraße 9a, 30167 Hannover, E-Mail: haberlandt@iww.uni-hannover.de

Abstract

Temporal rainfall disaggregation is an important tool to obtain high-resolution rainfall data which is needed in many fields of hydrology and water resources management. The multiplicative random cascade model can be used for temporal rainfall disaggregation of daily time series. A resampling algorithm is introduced to implement spatial consistence in disaggregated time series. Spatial consistence is assumed to be represented by four bivariate and distance-dependent rainfall characteristics that complement each other. Relative diurnal cycles of the disaggregated time-series are resampled with the aim to reproduce these spatial characteristics while preserving the structure generated by the cascade model. Also, to achieve a final resolution of 1 hour the traditional cascade model has been modified. A modification called uniform splitting with a branching number of 3 in the first step is introduced. Results are compared with observations and an approach by Güntner et al. (2001) called diversion. In total 22 recording stations in Northern Germany with hourly resolution were used for the validation of the disaggregation procedure, starting with daily values. Investigation areas are two catchments considering different station densities.

The results show that for the disaggregation, errors of time series characteristics between 3 % and 12 % occur. The non-exceedance curves of rainfall intensities are slightly overestimated. Extreme values are well represented. The uniform splitting method outperforms the diversion method. Spatial rainfall characteristics can be reproduced by the simulating annealing algorithm. However, with an increasing number of stations the reproduction performance declines for some rainfall characteristics. Non-exceedance curves of areal rainfall based on disaggregated and not resampled time series are generally underestimated. By application of the resampling algorithm, a better performance regarding the spatial characteristics can be achieved. The presented resampling algorithm has the potential to be used for implementing spatial consistence also for time series generated by other disaggregation models.

Introduction

Rainfall time series with a high temporal resolution are needed in many fields of hydrology and water resources management, e.g. urban hydrology (Licznar et al., 2011), flood risk assessment (Koutsoyiannis & Langousis, 2011) or erosion investigations (Jebari et al., 2012). In most cases these time series are short and the network density of the recording stations is low. Unfortunately, many applications require long time series and a dense network of rainfall stations.

Usually, non-recording station networks have a much higher density and a longer observation period. Time series information of the recording stations could be used to disaggregate those of the non-recording stations with the aim to produce a data set with long time series and a sufficient temporal resolution.

A method for disaggregation is the mutliplicative random cascade model, which was developed and applied originally in the field of turbulence theory (Mandelbrot, 1974). For rainfall disaggregation, the cascade model can be used either to increase the spatial resolution of rainfall fields (e.g. Gupta and Waymire, 1993) or to increase the temporal resolution (Olsson, 1998).

One problem with multiplicative cascade models for temporal disaggregation is their restriction to univariate cases, so that multisite application is not possible and has not been done so far to the authors' knowledge. The main objective of this work is to introduce a method for multisite applications considering spatial consistence in rainfall characteristics.

The disaggregation of time series without consideration of surrounding stations leads to unrealistic spatial patterns of rainfall. However, the existence of a spatial correlation of rainfall is indisputable and the question arises: how can spatial consistence be implemented after the disaggregation process? Simulated annealing is tested here, which is a resampling

algorithm, introduced for point rainfall generation by Bardossy (1998) and applied for multisite rainfall generation by Haberlandt et al. (2008). The idea is to resample relative diurnal cycles of the disaggregated time series under the restriction of keeping the structure constructed by the cascade model. The aim is to fulfil different spatial characteristics derived from observed time series. These characteristics are distance-dependent and bivariate and were former used in Wilks (1998), Haberlandt et al. (2008) and Breinl et al. (2013, 2014). The reproduction of spatial dependencies in the disaggregated time series is the first novelty of this investigation.

During recent years different types of cascade models have been developed, which can be classified in different ways. According to their principles of mass conservation, cascade models are divided into either micro-canonical or canonical cascade models. Micro-canonical models conserve the rainfall amount in each time step exactly, i.e. the initial time series could be reconstructed by aggregating the disaggregated time series. A second attribute of micro-canonical models regards parameter estimation. All parameters can be extracted directly from the data by a reverse application of the cascade model to the observations of recording stations (Carsteanu and Foufoula-Georgiou, 1996). Canonical cascade models on the other hand conserve rainfall amounts only on average for each time step. Only for the whole time series is an exact conservation achieved. A detailed comparison can be found in Lombardo et al. (2012). For these reasons, canonical cascade models belong to downscaling methods and micro-canonical models to disaggregation methods (Koutsoyiannis and Langousis, 2011).

Another classification is according to the scale-dependency of parameters used in the cascade model. Bounded cascade models (Marshak et al., 1994) use a special parameter set for each cascade level. Due to this, the random process becomes smoother on smaller time scales. For unbounded cascade models, one parameter set is applied independently of the cascade level

93 under the assumption of parameter scale-invariance in a certain range. A discussion about
94 scale-dependency of the parameters can be found in Serinaldi (2010). Although
95 Veneziano et al. (2006) identified scale-dependency, Rupp et al. (2009) showed only a slight
96 improvement using scale-variant parameters if the cascade model is applied over a small
97 range of disaggregation levels. One advantage of scale-invariance is the possibility to estimate
98 the parameters by aggregation of the time series which are used for later disaggregation.

99 The branching number *b* in a cascade model gives the number of finer time steps to which the
100 rainfall is distributed from one coarser time step. The choice of parameter scale-dependence
101 determines in combination with the branching number *b* the number of parameters for the
102 cascade model. An unbounded cascade with *b=2* is the most parameter parsimonious version
103 of the cascade model. However, the final temporal resolution of 1.5 or 0.75 hours if starting
104 with daily values can be a problem, since a wide variety of applications need hourly input.
105 Güntner et al. (2001) tried to overcome this issue with a diversion at the 5^{th} disaggregation
106 level (0.75 h) into three time intervals and subsequently aggregating four of the intervals into
107 hourly values. However, this destroys the structure created by the cascade model, although
108 results look satisfactory for the investigated data. Lisniak et al. (2013) have chosen a
109 branching number *b=3* for the first disaggregation step which continues to resolutions of 8, 4,
110 2 and 1 h. Their cascade model was bounded and parameters were additionally estimated for
111 different atmospheric circulation patterns. This resulted in a high number of parameters
112 giving better performance for a calibration period using the circulation pattern, but with no
113 improvement for the validation period.

114 Another research question of this study is: how might the cascade model be extended to
115 derive hourly time series starting from a source of daily values and yet still retaining the
116 cascade structure intact? A possible answer to this question is the second novelty of our study.

We introduce a more parameter parsimonious alternative for rainfall disaggregation to obtain the aspired temporal resolution by applying the structure of a cascade model.

The paper is organized as follows. In section 2 the investigation area and rainfall stations are described. In section 3 the applied methods are discussed, whereby the first part includes the possibilities of rainfall disaggregation to derive hourly time steps. The second part concerns the implementation of spatial consistence in these time series. In section 4 the results for both time series disaggregation and resampling algorithm are shown and discussed. Summary and outlook are given in section 5.

Data

The stations used for this investigation are located in and around the Aller-Leine river basin (15703 km², see Fig. 1) which covers a large southern portion of the federal state of Lower Saxony in Germany. The river basin can be divided into two different regions, the flatland around the Lüneburger Heide in the north and the Harz middle mountains in the south. The Harz mountains have altitudes up to 1141 m and areas with average annual precipitation greater than 1400 mm. According to the Köppen-Geiger climate classification, a temperate oceanic climate exists in the north of the study area, while a temperate continental climate exists in the south (Peel et al., 2007). Additionally, the Upper Leine catchment located in the south of the study area with a size of 992 km² is considered. This is the headwater subcatchment of the Aller-Leine river basin.

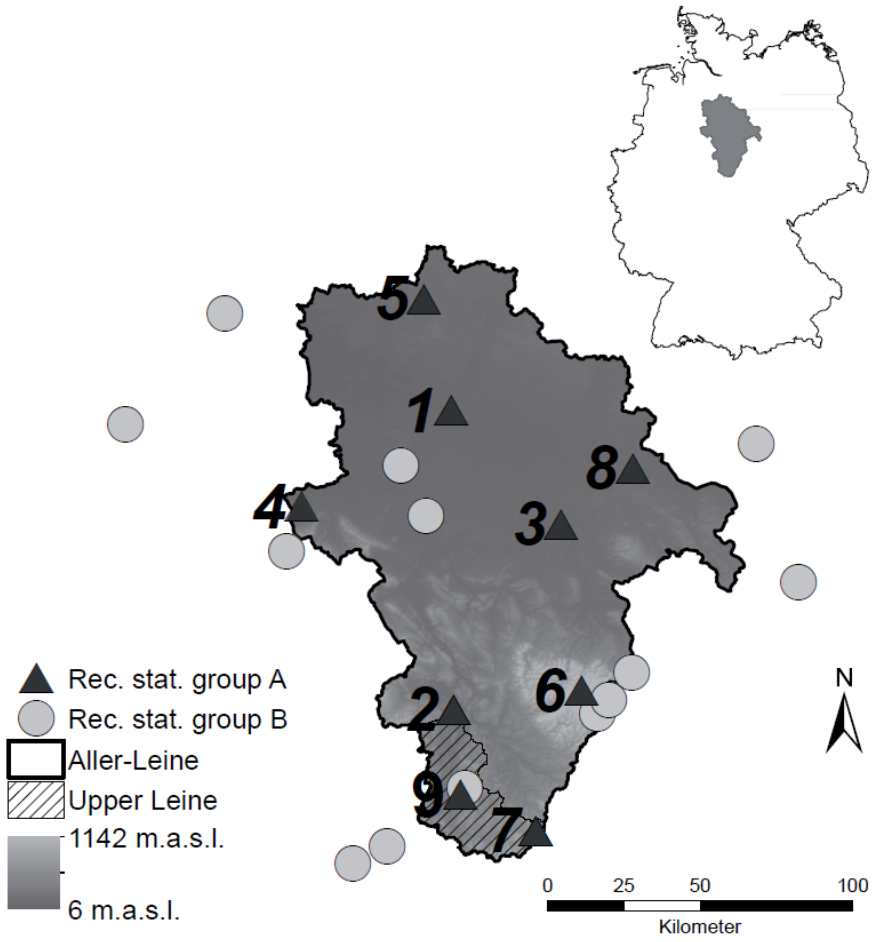

Fig. 1. Location of the Aller-Leine river basin with Upper-Leine subcatchment, recording rainfall stations and topography. The location of the river basin within Germany is shown in the upper right map.

In Fig. 1, 22 recording stations (group A and B) from the German Weather Service DWD and Meteomedia AG are shown. For these stations long time series with a temporal resolution of one hour or finer are available. Recording stations of group A are rainfall stations used during the resampling procedure. For the validation of the resampling process it would be optimal to have time series with almost no missing values. A uniform time period from 15 December 2002 to 30 January 2007 was used. Recording stations of group B were used additionally for the estimation of spatial rainfall characteristics described in section 3. For the description of the time series, overall characteristics like average intensity and fraction of wet hours, but also event characteristics like dry spell duration, wet spell duration and wet spell amount, are used.

149 Events are defined by a minimum of one dry hour before and after the rainfall occurrence.
150 These characteristics and further information of the rainfall stations of group A are given in
151 Table 1. If for any other purpose different time series lengths are used it is mentioned in the
152 text.

153 Table 1. Attributes of rainfall stations of group A and time series characteristics for a temporal resolution of
154 1 hour

Name	Short ID	Altitude [m.a.s.l.]	Mean annual precipitation [mm]	Fraction of wet hours [%]	Average wet spell duration [h]	Average wet spell amount [mm]	Average dry spell duration [h]	Average intensity [mm/h]
Hambuehren	1	38	635.0	11.1	2.7	1.9	17.9	0.70
Wetze/Northeim	2	122	642.7	12.3	2.5	1.7	19.5	0.67
Braunschweig-Voel.	3	81	607.7	10.0	2.4	1.9	23.3	0.79
Stadthagen	4	62	622.6	11.1	2.4	1.7	17.3	0.71
Soltau	5	76	799.6	18.1	3.2	2.0	18.3	0.63
Torfhaus (Harz)	6	805	1 325.9	10.9	3.7	3.2	15.3	0.86
Leinefelde	7	356	734.5	8.8	2.6	2.0	20.5	0.78
Wolfsburg-Autostadt	8	61	591.3	14.5	2.5	1.7	21.6	0.68
Göttingen	9	167	637.7	11.7	2.7	1.7	19.7	0.63

155

156 **Methods**

157 To provide an overview of the applied methods and resulting data sets, the general steps of
158 the study are presented as a flow chart in Fig. 2. Observed time series are disaggregated with
159 two modifications of the cascade model: diversion (DIV) and uniform splitting (US) (see
160 3.1). The disaggregated time series are resampled with a simulated annealing algorithm (see
161 3.2). Hereby a one-step and a two-step approach exist. The two-step approach is only applied
162 for the Aller-Leine river basin.

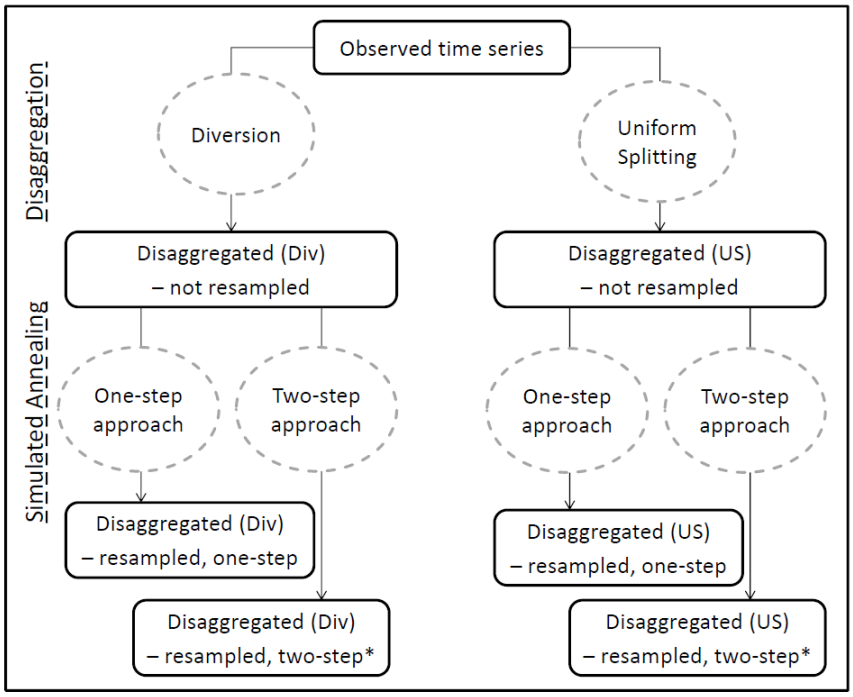

Fig. 2. Flowchart of the applied methods, their modifications (in circles) and resulting datasets (boxes). Data sets indicated by a * are only derived for the Aller-Leine river basin

Cascade Model

The principle of the cascade model is illustrated in Fig. 3. A time step from a coarser time level is disaggregated into two finer time steps of equal duration. The number of boxes generated from the coarser time level is called the branching number, which here is $b = 2$. In this investigation, a micro-canonical, unbounded cascade model is used (see Sect. 1).

The rainfall volume V of the coarser time step is multiplied with the multiplicative weights W_1 and W_2 to obtain the rainfall volumes of the finer time step. The sum of W_1 and W_2 is equal to 1 in each split, i.e. they are not independent of each other. Overall there are three possibilities of how the rainfall volume can be split (Eq. (1)) during the disaggregation:

$$W_1, W_2 = \begin{cases} 0 \text{ and } 1 & \text{with P}(0/1) \\ 1 \text{ and } 0 & \text{with P}(1/0) \\ x \text{ and } 1-x & \text{with P}(x/(1\text{-}x));\ 0<x<1 \end{cases}, \quad (1)$$

where P is the probability for each splitting. A splitting with the probability $P(1/0)$ means that the whole rainfall is assigned to the first time step ($W_1 = 1$) and no rainfall ($W_2 = 1 - W_1 = 0$) is assigned to the second time step. With the probability $P(0/1)$, splitting is achieved vice versa. The third possibility is a $x/(1-x)$-splitting that redistributes the rainfall volume over both time steps. Here x is defined as $0 < x < 1$ and represents the relative fraction of the rainfall volume which is assigned to the first time step. Considering x as a random variable for all disaggregation steps, a probability density function $f(x)$ with the probabilities for each value of x can be estimated.

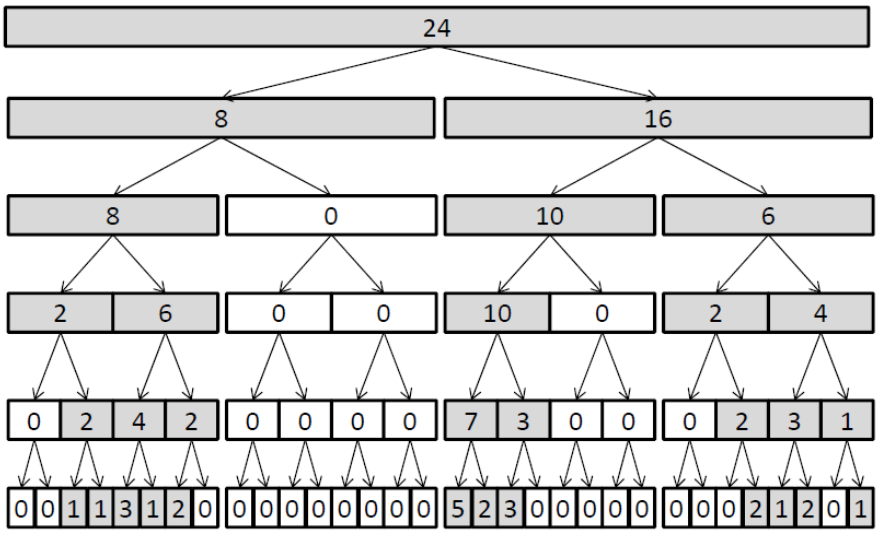

Fig. 3. Multiplicative cascade model (after Olsson, 1998)

Given $f(x)$ and the three probabilities $P(0/1)$, $P(1/0)$ and $P(x/(1-x))$, the basic version of the cascade model requires only four parameters. Olsson (1998) and Güntner et al. (2001) identified parameter dependencies on the position and the rainfall volume of each time step.

Position of a time step is the relation to the wetness of the neighboring time steps and was used before by e.g. Buishand (1977). Olsson (1998) introduced a differentiation into four classes, which was adopted by other authors (e.g. Lisniak et al., 2013): Starting boxes

194 (preceded by a dry time step, succeeded by a wet time step~dry-wet-wet), enclosed boxes
195 (wet-wet-wet), ending boxes (wet-wet-dry) and isolated boxes (dry-wet-dry).

196 In addition, the rainfall volume of a time step is considered. Olsson (1998) assumed that the
197 parameters differ for higher and lower volumes and determined for every position class a
198 volume threshold to create two volume classes. The chosen threshold was the mean rainfall
199 over all time steps of this position. Güntner et al. (2001) tested the median as a more suitable
200 volume threshold. The advantage of using the median is that the number of occurrences in
201 both volume classes will be equal. However, using the mean led to better results and hence
202 was used here.

203 For *f(x)*, empirical distribution functions were used. According to Güntner et al. (2001), an
204 acceptable fitting of theoretical distribution functions is barely possible for every combination
205 of position-volume-classes.

206 Altogether the model uses 32 parameters (4 basic parameters · 4 position classes · 2 volume
207 classes). For this study, these parameters were estimated by aggregating high-resolution time
208 series and counting the number of occurrences for the different types of splitting for each
209 volume-position-class. The estimation of *f(x)* was carried out similarly. In general, no high-
210 resolution time series exist at the point of interest, therefore the parameters must be estimated
211 in a different way. One solution is to estimate the parameter set at the nearest station and then
212 apply the parameter set at the point of interest (Koutsoyiannis et al., 2003). If the parameters
213 are supposed to be independent from scale, they can also be estimated by aggregating the
214 daily values at the point of interest and then applied for disaggregation of these daily values.

215 The disaggregation procedure using the multiplicative cascade model with a branching
216 number $b = 2$ and starting with daily values, results in a temporal resolution of 1.5 h or
217 0.75 h. However in most cases hourly rainfall data is needed. Güntner et al. (2001) analyzed

218 different methods to derive a final temporal resolution of 1 h. To overcome this problem they
219 tested different variants and identified the "diversion" (called the $E_{24/0.75/1}$-experiment) to
220 deliver best results. For the diversion, time steps at the 5th disaggregation level ($\Delta t = 0.75$ h)
221 are split uniformly into three time steps with $\Delta t = 0.25$ h, and afterwards four of these time
222 steps are aggregated to achieve a final resolution of $\Delta t = 1$ h.

223 Here, another variant similar to Lisniak et al. (2013) is introduced, the so called "uniform
224 splitting". Starting at a daily time scale in the first disaggregation step, a branching number of
225 $b = 3$ is chosen. Additionally needed parameters are the probabilities for one ($P(0/0/1)$) and
226 for two wet intervals ($P(0/\frac{1}{2}/\frac{1}{2})$) of the three 8 h-intervals of a day. The probability for three
227 wet 8 h-intervals can be determined by $P(\frac{1}{3}/\frac{1}{3}/\frac{1}{3}) = 1-P(0/0/1)-P(0/\frac{1}{2}/\frac{1}{2})$. The following
228 assumptions were made:

229 1. The parameter $P(0/0/1)$ and $P(0/\frac{1}{2}/\frac{1}{2})$ influence only the number of wet boxes, not
230 their position. The position of each wet box is assigned randomly.

231 2. The rainfall volume is uniformly split to all boxes which are defined as wet.

232 The possibilities of splitting during the first disaggregation step are shown in Eq. (2):

$$W_1, W_2, W_3 = \begin{cases} 1, 0 \text{ and } 0 & \text{with P(0/0/1)} \\ 0, 1 \text{and } 0 & \text{with P(0/0/1)} \\ 0, 0 \text{ and } 1 & \text{with P(0/0/1)} \\ \frac{1}{2}, \frac{1}{2} \text{ and } 0 & \text{with P}(0/\frac{1}{2}/\frac{1}{2}) \\ \frac{1}{2}, 0 \text{ and } \frac{1}{2} & \text{with P}(0/\frac{1}{2}/\frac{1}{2}) \\ 0, \frac{1}{2} \text{ and } \frac{1}{2} & \text{with P}(0/\frac{1}{2}/\frac{1}{2}) \\ \frac{1}{3}, \frac{1}{3} \text{ and } \frac{1}{3} & \text{with P}(\frac{1}{3}/\frac{1}{3}/\frac{1}{3}) \end{cases} \quad (2)$$

For the second and all following disaggregation steps, $b = 2$ is used, so that time series with resolutions of 4 h, 2 h and 1 h are produced.

The additional parameters can be estimated by aggregating recording stations, e.g. starting at $\Delta t = 1$ h leads, to 2 h, 4 h and 8 h. The probabilities $P(\frac{1}{3}/\frac{1}{3}/\frac{1}{3})$, $P(0/\frac{1}{2}/\frac{1}{2})$ and *P(0/0/1)* are the same for starting, enclosed, ending and isolated positions.

In contrast, the separation into volume classes is retained. Without a second volume class, the probability *P(0/0/1)* is the same for both small and high rainfall amounts in a day. Fig. 4 shows the number of wet 8 h-intervals of a day in relation to the daily rainfall amount for two stations with a time series length of approximately 18 years. It can be seen that for higher daily rainfall amounts, the probability of a higher number of wet 8 h-intervals increases.

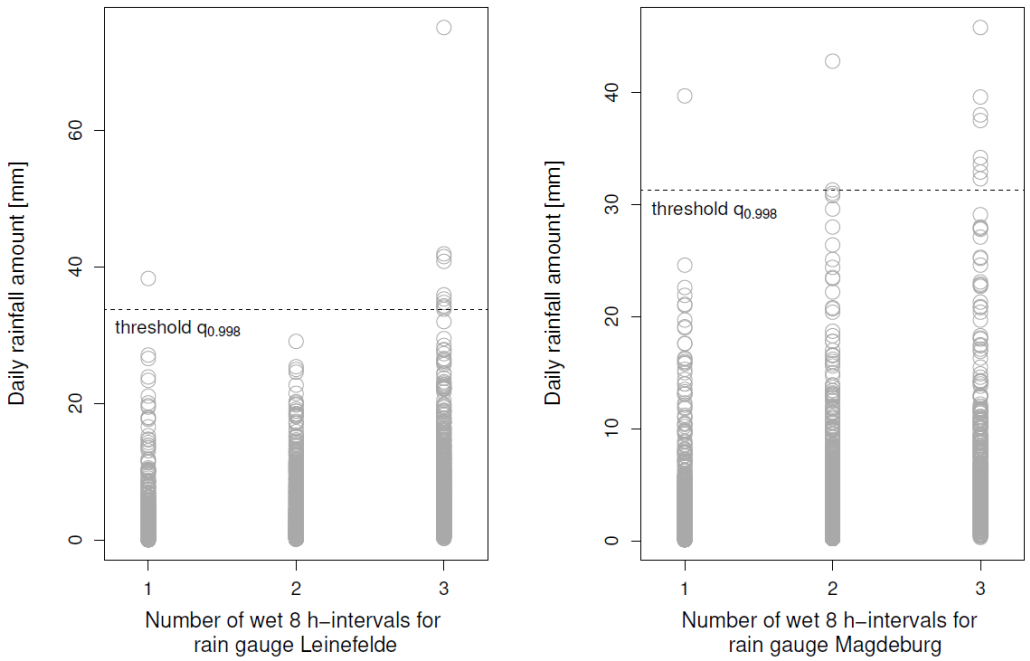

Fig. 4. Daily rainfall amount and corresponding number of wet 8 h-intervals for the rain gauges Leinefelde and Magdeburg. The red line is the volume threshold defined as the quantile $q_{0.998}$.

For this study a quantile $q_{0.998}$ was chosen as volume threshold. The quantile was identified in a way to represent the different probability of wet 8 hours-intervals of the two volume classes. The probabilities $P(\frac{1}{3}/\frac{1}{3}/\frac{1}{3})$, $P(0/\frac{1}{2}/\frac{1}{2})$ and *P(0/0/1)* of the upper and lower volume class differ strongly using this calibrated threshold.

For the evaluation of diversion and uniform splitting, time series of recording stations were aggregated to daily values. The disaggregation products of these two methods were computed and then compared to the observed time series with 1 h-resolution. The disaggregation is a random process and, depending on the initialization of the random number generator, leads to different results. To cover this random behavior, a certain number of disaggregation runs has to be performed. We found, that after 80 disaggregation runs the average values of the main characteristics (see Table 3) are not changing significantly by an increasing number of disaggregation runs. Accordingly, 80 disaggregations were carried out for each method.

Table 3. Relative error of characteristics for all recording stations of group A using diversion (Div) and uniform splitting (US) in comparison with characteristics of observed time series (based on 80 disaggregations for each method and station)

Rainfall characteristic	r [%]		RRSE [%]		MAE	
	Div	US	Div	US	Div	US
wet spell duration [h]	**40**	**-12**	**43**	**17**	**1.1**	**0.5**
standard deviation	12	-29	25	30	0.7	0.9
skewness	-32	-26	32	27	1.3	1.1
wet spell amount [mm]	**12**	**-9**	**26**	**16**	**0.5**	**0.4**
standard deviation	-4	-18	17	24	0.8	1.1
skewness	-19	-19	22	22	1.4	1.4
dry spell duration [h]	**10**	**-6**	**15**	**12**	**2.6**	**2.3**
standard deviation	6	-7	11	11	4.1	4.5
skewness	-5	9	8	10	0.4	0.5
fraction of dry intervals	**-7**	**-3**	**5**	**3**	**0.0**	**0.0**
average intensity [mm/h]	**-20**	**4**	**20**	**9**	**0.1**	**0.1**

Implementing spatial consistence using resampling

The multiplicative random cascade model is disaggregating the time series of one rainfall station without consideration its spatial relationship with surrounding stations. This would lead to errors in areal rainfall estimation if precipitation is used for instance as input for hydrological models. Spatially connected rainfall events are disaggregated and take place at different time steps at different stations, so areal rainfall is assumed to be underestimated. The main idea is to resample relative diurnal cycles using a simulated annealing algorithm (Kirkpatrick et al., 1983; Aarts and Korst, 1965) to implement spatial consistence. Simulated annealing is a non-linear optimization method that minimizes an objective function with the ability to find the global minimum.

First it has to be defined which criteria can be used in the objective function to describe the spatial characteristics of rainfall time series z. For this purpose the following three bivariate characteristics were chosen, which can be calculated from hourly rainfall time series:

1. Probability of occurrence

The first characteristic $P_{k,l}$ describes the probability of rainfall occurrence at two stations k and l at the same time:

$$P_{k,l}\left(z_k > 0 \mid z_l > 0\right) \approx \frac{n_{11}}{n} \quad , \tag{3}$$

where n is the total number of non-missing observation hours at both stations k and l, and n_{11} represents the number of simultaneous rainfall occurrence at both stations.

2. Pearson's coefficient of correlation

To describe the relationship between simultaneously occurring rainfall at two stations k and l the Pearson's coefficient of correlation is used, which is a measure of the linear relation between both rainfall time series (Eq. (4)). This coefficient was used for e.g. multisite rainfall generation before by Breinl et al. (2014):

$$\rho_{k,l} = \frac{cov(z_k, z_l)}{\sqrt{var(z_k)\, x\, var(z_l)}} \text{, } z_k > 0, z_l > 0 \quad . \tag{4}$$

3. Continuity measure

The third bivariate characteristic is the continuity measure according to Wilks (1998). It compares the expected rainfall amount at one station for times with and without rain at the neighbouring station (E. is the expectation operator):

$$C_{k,l} = \frac{E(z_k | z_k > 0, z_l = 0)}{E(z_k | z_k > 0, z_l > 0)} \quad . \tag{5}$$

It is possible to estimate prescribed values of these characteristics as functions of the separation distance between two stations from observed data. For the Aller-Leine catchment, these characteristics were estimated for all available stations of group A and B. For the

parameter estimation the full length of all time series were used, not only the simultaneous observation period. The results are shown in Fig. 5.

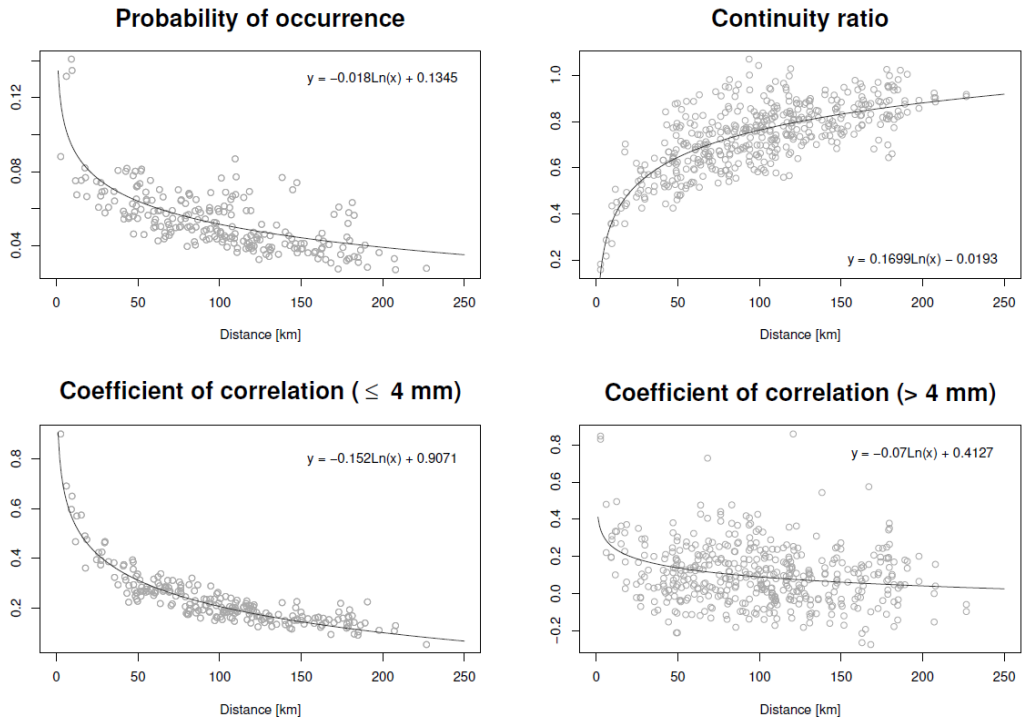

Fig. 5. Estimated spatial characteristics as functions of the separation distance with regression lines used as input for the objective function (please note the different scale of y-axis for the two coefficients of correlation)

The correlation coefficient depends strongly on the analyzed rainfall volumes for the investigated time series. Fig. 5 shows the correlation for values below and above a threshold of 4 mm. The value of 4.0 mm was identified as the threshold at which the spatial correlation becomes very weak. Since lower rainfall volumes are supposed to originate from advective rainfall events with large spatial extensions, their spatial correlation is much stronger than for higher rainfall volumes, which may occur during convective rainfall events with a limited spatial extension. Hence, two correlation coefficients for values below ($\rho_{k,l,\leq 4\ mm}$) and above 4 mm ($\rho_{k,l,>4\ mm}$) were used.

In order to define prescribed values for the objective function suitable functions are required to relate these characteristics to the distance. Here, logarithmic regression curves give the highest coefficient of determination and are chosen for all three characteristics.

All four characteristics are summarized in a bivariate objective function:

$$O_{k,l} = w_1 \times \left(P_{k,l} - P^*_{k,l}\ *\right) + w_2 \times \left(\rho_{k,l,\leq 4} - \rho^*_{k,l,\leq 4}\right) + w_3 \times \left(\rho_{k,l,>4} - \rho^*_{k,l,>4}\right) + w_4 \times \left(C_{k,l} - C^*_{k,l}\right) \quad (6)$$

The parameters indicated by * are the prescribed values for two stations, and the other parameters are the actual values. The weights w_1, w_2, w_3 and w_4 are necessary to consider the importance and to adjust the scale of the rainfall characteristics.

After disaggregation, the time series with an hourly resolution have to be resampled to implement spatial consistence. There are two conditions which need to be considered for resampling:

1. The structure of the disaggregated time series should be conserved, with different position and volume classes produced by the cascade model.

2. The rainfall amount of each day should be conserved. One advantage of the micro-canonical cascade model is the exact conservation of mass in each time step. Hence a swap of absolute values between two days is not possible.

The aim of the simulated annealing is to modify all disaggregated and unchanged time series N (called set U) under the above mentioned conditions to receive disaggregated, changed time series with spatial consistence (called set R). Simulated annealing is carried out as follows:

1. For time series $k=1,\ldots, N$, relative diurnal cycles of each wet day are constructed. The relative diurnal cycles are split into x subsets, with $x=1,\ldots, S$ for each combination of position and volume class, In case of the uniform splitting an additional subset for all values above $q_{0.998}$ exists.
2. A time series k from set U is drawn randomly. If set U is empty the procedure is ended.
3. All time series from set R with $l=1,\ldots, M$ are taken as reference time series. If set R is empty, time series k is moved from the set U to set R and the algorithm returns to step 2, otherwise it proceeds to step 4.
4. A subset x of k is identified randomly, where every subset with its number of elements m has the probability:

$$P_{x,i}=\frac{m_i}{\sum_{m=1}^{S} m_i} \quad (7)$$

5. Two days are drawn randomly from the subset identified in step 4 and their diurnal cycles are swapped.
6. The value for the objective function $O_{k,l}$ (Eq. (6)) is updated. An average objective function value O_k is calculated considering all neighboring stations from set R:

$$O_k = \frac{1}{k-1}\sum_{l=1}^{M} O_{k,l} \quad (8)$$

7. The new value of the objective function is compared with the former value obtained before the actual swap. The swap is accepted if $O_{new} < O_{old}$.
8. If $O_{new} \geq O_{old}$ the swap is accepted with the probability π:

$$\pi = \exp\left(\frac{O_{old}-O_{new}}{T_a}\right), \quad (9)$$

where T_a is the annealing temperature. This parameter regulates the probability of accepting bad swaps. By the acceptance of bad swaps local optima can be avoided as final solution and the global optimum can be identified. Decreasing this parameter during the simulated annealing procedure (see further steps) the probability for accepting non-improving swaps is also decreasing, allowing a convergence to a global optimum.

9. Steps 4-8 are repeated *K* times.
10. The annealing temperature is reduced by:

$$T_a = T_a \times dt \qquad \text{with } 0 < dt < 1 \tag{10}$$

After reducing the temperature, the algorithm proceeds to step 4.

11. Steps 9 and 10 are repeated until the algorithm converges regarding resampling of the station *k*.
12. Station *k* is removed from set *U* and added to set *R*. The algorithm returns to step 2 for resampling the next station.

The algorithm explained above is theoretically not limited to a certain number of stations. However, with an increasing number of stations, it becomes more difficult to reach a final small objective function value. Every new disaggregated time series from set *U* has to be fitted to all already resampled time series from set *R*. Due to the limited amount of available diurnal cycles, a good fitting becomes increasingly difficult with every newly added time series. An overview of the number of diurnal cycles for station 3169 is given in Table 2. For the upper volume class of the isolated boxes, only 28 diurnal cycles are available to swap, which is a very low number in comparison to the amount of diurnal cycles of lower volume classes for all positions. This poses a serious problem if a large area with many stations needs to be considered. With an increasing areal extension of the study area, the scale and the

purpose of the areal rainfall has to be questioned. For some applications, a good fit between all rainfall stations, some of them situated remotely from each other, may not be essential, and a resampling of the rainfall time series of a single subcatchment or small groups would be sufficient.

A possible solution could be the application of a multi-step approach, also called a nested approach proceeding from large to small scales. Hereby a subset of all time series is resampled in a first step. In a second step, the already resampled stations are used as reference time series (so k_1 is fixed) and other, non-resampled stations will be resampled following the 11-point-scheme described before.

Table 2. Number of diurnal cycles for each position and volume class for station 3169

Position	Volume class	
	Lower	Upper
Starting	126	52
Enclosed	205	114
Ending	124	54
Isolated	84	28

For a better understanding, the station IDs from Fig. 1 are used to illustrate the method. In the first step, a subset *U1={*station 1, 2, 3} is chosen from set *U*={1, 2, 3, 4, 5, 6, 7, 8} representing the large scale. The stations were chosen to cover all parts of the study area, the North (station 1), the South (station 2) and the East (station 3). This subset is used instead of set *U* in the resampling procedure. The resampled time series of these stations are used as donor time series for nearby stations in the next step focusing on smaller scales.

For the second step, the resampled time series of set *R*={1, 2, 3} are distributed on *t* new subsets *U1-t*, where *t* is the number of elements of the set *R* (*t* = 3). To every new subset *U1-t*, disaggregated, not resampled time series are added (*U1-1* = {1, 4, 5}, *U1-2* = {2, 6, 7}, *U1-3* = {3, 8}). For every subset *U1-t*, the resampling procedure is applied independently from

401 the other subset with the restriction that the already resampled time series from set *R* is the
402 reference used during the simulated annealing (k_1 = 1 for *U1-1*, k_1=2 for *U1-2*, k_1=3 for *U1-*
403 *3*)). This approach could be continued for more steps, but here only a two-step approach is
404 applied.

405 For the estimation of the areal rainfall, the inverse distance method was chosen. This method
406 is based on the assumption that rainfall from two stations with a closer distance is more alike.
407 Accordingly, the interpolation result is a linear combination of surrounding observations with
408 weights being inversely proportional to the square distance between the observations and the
409 point of interpolation (Goovaerts, 2000).

410

411 **Results & Discussion**

412 **Rainfall characteristics of point disaggregation**

413 For the rainfall disaggregation, two versions of the cascade model were analyzed: diversion of
414 Güntner et al. (2001) and uniform splitting. A comparison of the characteristics of
415 disaggregated time series (*Dis*) using both methods with the observations (*Obs*) can be seen in
416 Table 3 regarding the relative error *r* (11), the root relative squared error *RRSE* (12) and the
417 mean absolute error *MAE* (13). The objective criteria were calculated for each station over all
418 realizations *n* of the disaggregation and averaged afterwards over all stations.

419 $$r = \frac{1}{n} \times \sum_{i=1}^{n} \frac{(r_{Dis,i} - r_{Obs})}{r_{Obs}} \quad (11)$$

420 $$RRSE = \frac{1}{n} \times \sum_{i=1}^{n} \sqrt{\left(\frac{(RRSE_{Dis,i} - RRSE_{Obs})}{RRSE_{Obs}}\right)^2} \quad (12)$$

421 $$MAE = \frac{1}{n} \times \sum_{i=1}^{n} |MAE_{Dis,i} - MAE_{Obs}| \quad (13)$$

All three objective criteria lead to similar relations between the results for diversion and uniform splitting. For the further interpretation only the relative error is used, since this criterion has the advantage to draw conclusions about over- or underestimation of the rainfall characteristics.

For the diversion, the average wet and dry spell durations are overestimated by 40 % and 10 % respectively. The average intensity is underestimated by 20 %. This could be caused by the last two steps of the diversion approach. In some cases the duration of wet intervals is extended by the elimination of short dry periods. Due to the reduction and removal of short dry intervals, both event characteristics are overestimated. These results are comparable to Güntner et al. (2001), who found for Brazilian stations an overestimation of wet spell duration, but only by 10 %, instead of the 40 % in this study. The smaller error could be caused by the mean dry spell duration that was much longer for Brazilian time series. Although wet and dry spell durations are overestimated, only small deviations can be recognized for the fraction of dry intervals of the whole time series.

Uniform splitting only slightly underestimates wet and dry spell durations by 12 % and 6 % respectively. One reason could be the random positions of the wet 8 h-intervals in a day which causes artificial small rainfall events with dry periods in between, which are shorter than the mean observed dry spell duration. Average rainfall intensities are overestimated and the fraction of dry intervals are underestimated, both by less than 5 %.

In addition to the basic event characteristics of the time series, non-exceedance curves of rainfall intensity based on hourly time steps were analyzed. Therefore, all wet hours from 80 disaggregations using diversion and uniform splitting were extracted and plotted as non-exceedance curves in Fig. 6. Furthermore, the observed values for station Wetze/Northeim are displayed. It can be seen that the diversion underestimates the observations in the range from

0 % to 98 %. This represents hourly rainfall amounts up to about 4 mm and is indicated by an average underestimation of 20 % of the average rainfall intensity. Uniform splitting shows a good fit from 35 % to 93 %, which represents the range from 0.1 mm to 2 mm. Higher values of rainfall amount are overestimated.

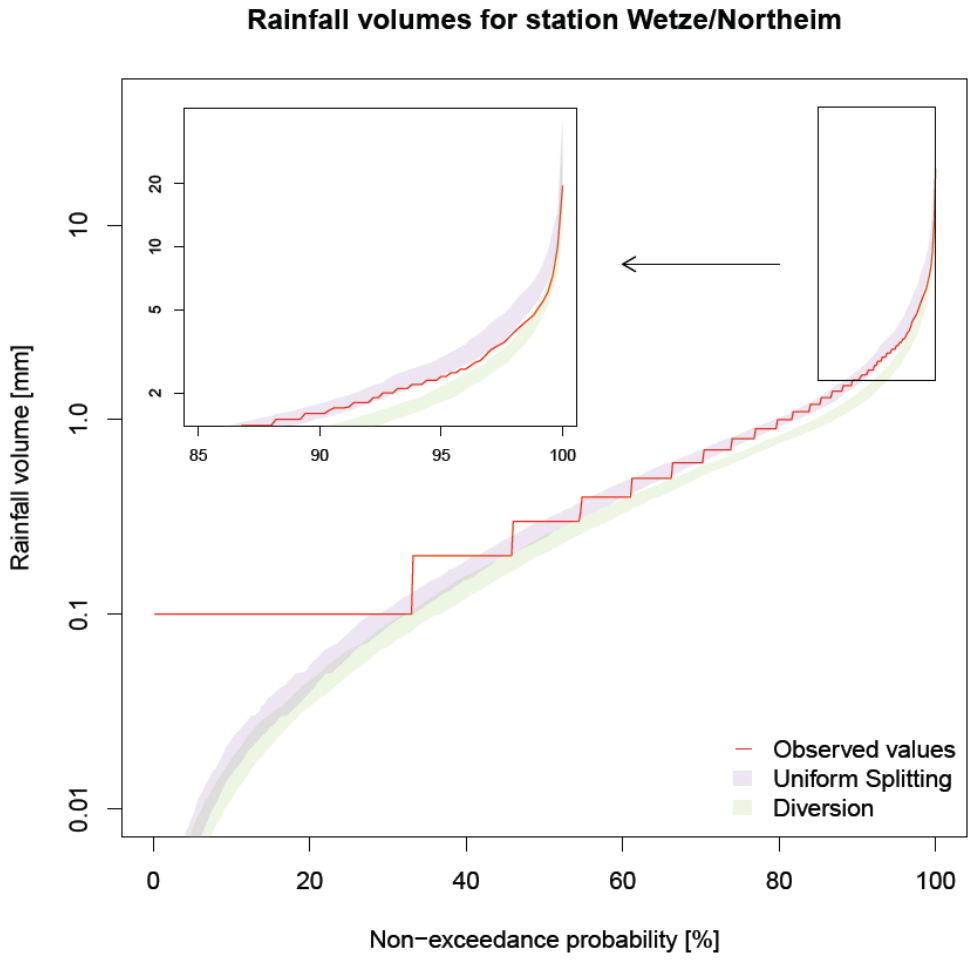

Fig. 6. Non-exceedance curves of observed and disaggregated time series for station Wetze/Northeim, with a detailed look at the upper 15 % of non-exceedance curve in the upper left corner. The shaded areas represent the enveloping curves of all 80 realizations for each method.

The underestimation of observed rainfall amounts in the range from 0 % to 35 % results from the resolution of the measuring instruments. Hence, the lowest observed rainfall value is 0.1 mm. From the observed data it can be seen that these very small values represent one third

458 of all values. These values can be represented neither by the diversion nor by the uniform
459 splitting method. The results for other stations look similar, so only station Wetze/Northeim is
460 presented here. Molnar & Burlando (2005) found the same problem, with 48 % of all wet
461 values smaller than the measuring accuracy of 0.1 mm for 10 minute data. This higher
462 fraction may have resulted from additional disaggregation steps that are necessary to achieve
463 the finer temporal resolution. To avoid this high occurrence of small values, a threshold could
464 be introduced like e.g. the sampling resolution of a measurement device. However, this would
465 require a complete new cascade generator with new parameters and will therefore be left for
466 further research. Also, low intensity rainfall periods are not important from a practical point
467 of view (Molnar & Burlando, 2005). It remains unclear if there are too many small values
468 produced or if the accuracy of the measurement instrument is causing too many dry periods
469 (Koutsoyiannis et al., 2003).

470 Additionally, rainfall extremes of the disaggregated time series were analyzed. For an analysis
471 of extreme values, long time series are necessary. Therefore the complete observation periods
472 were used. For each year only the highest value is taken into account and empirical non-
473 exceedance curves are calculated using the plotting position after Weibull (1939).

474 Fig. 7 shows the observed extreme values and the enveloping curves of 80 disaggregations for
475 the diversion and uniform splitting approach for two stations. The observed extreme values
476 are enveloped by both disaggregation methods over the whole spectrum. The diversion tends
477 to underestimate observed extremes for non-exceedance probabilities by up to 80 %. In
478 contrast, the uniform splitting tends to overestimate extreme values. The upper 20 % of
479 extreme values of station Göttingen are well represented by the median of all 80 diversion
480 realizations while the median of the uniform splitting tends to underestimate these extremes.
481 For station Hannover-Langenhagen the situation is reversed. However, extremes are in the

range of the 80 disaggregations for both methods. The ranges of the diversion and uniform splitting are similar from between 0 % to 70 % non-exceedance probability. The maximum range of the diversion is approximately 3 times wider than for the range of the uniform splitting.

In summary, the uniform splitting better reproduces basic event characteristics, the non-exceedance curve of rainfall intensities and the representation of extreme values than does the diversion.

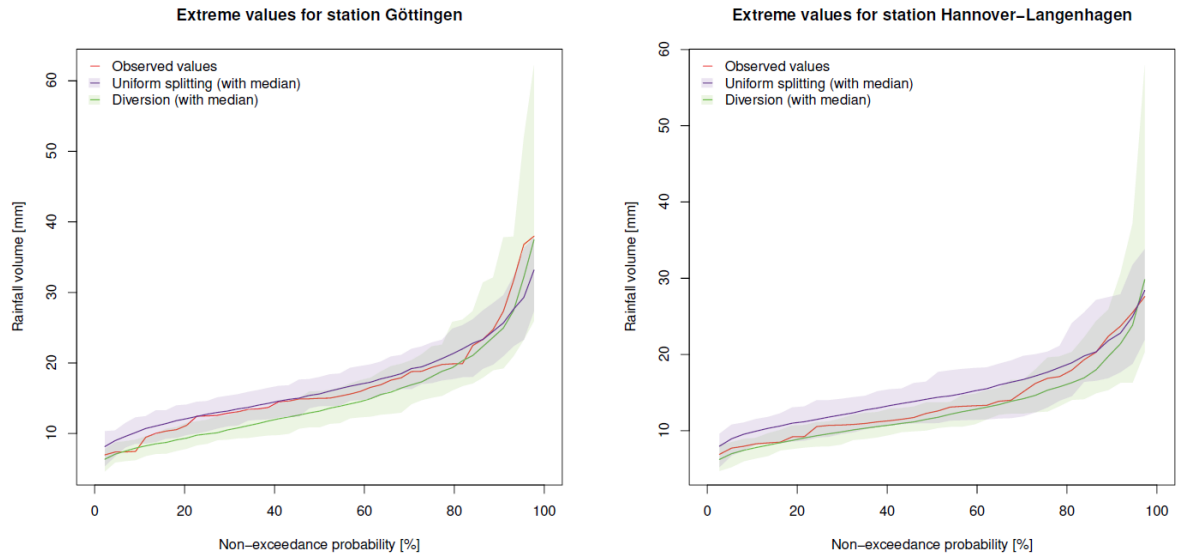

Fig. 7. Non-exceedance curves of rainfall extreme values with empirical probability for station a) Göttingen (43 years, 1951-2007 with missing values from 1981-1993) and b) Hannover-Langenhagen (36 years, 1959-2007 with missing 1981-1992). The shaded areas represent the enveloping curves of all 80 realizations for each method, the solid line represents the median.

Spatial rainfall characteristics

The implementation of spatial consistence should conserve the time series structure and basic event characteristics generated by the cascade model. Due to the applied resampling procedure and its boundary conditions, neither the structure defined as the arrangement of wet

499 days with different position-volume-classes, nor the rainfall characteristics of Table 3, have
500 been changed.

501 To evaluate the implementation of spatial consistence, spatial rainfall characteristics
502 (probability of occurrence, coefficient of correlation ($k \leq$ and > 4 mm) and continuity ratio)
503 were analyzed. Since all of them are included in the objective function, a general
504 improvement could be achieved. For this discussion, the term 'observation cloud' is
505 introduced. The observation cloud represents all values computed from the observed values
506 for each spatial characteristic.

507 A comparison of spatial characteristics before and after using simulated annealing is shown in
508 Fig. 8 for the one-step and the two-step approach. Values of the spatial characteristics are
509 illustrated for observed (grey), disaggregated (blue) and disaggregated and resampled (red)
510 time series. For the disaggregation, uniform splitting was applied. The overall aim of the
511 simulated annealing is to implement spatial characteristics, so that after resampling, values
512 should be in the cloud of observed values and show a dependence with distance. Reaching the
513 regression line of observations is not necessarily essential, since it is only a supporting tool
514 for the implementation of the characteristics in the objective function. For the annealing
515 algorithm, 3 out of the 80 realizations were chosen at random. Simulated annealing was
516 carried out 3 times each, so the data represents 9 data sets for the one-step approach and 27
517 data sets for the two-step approach.

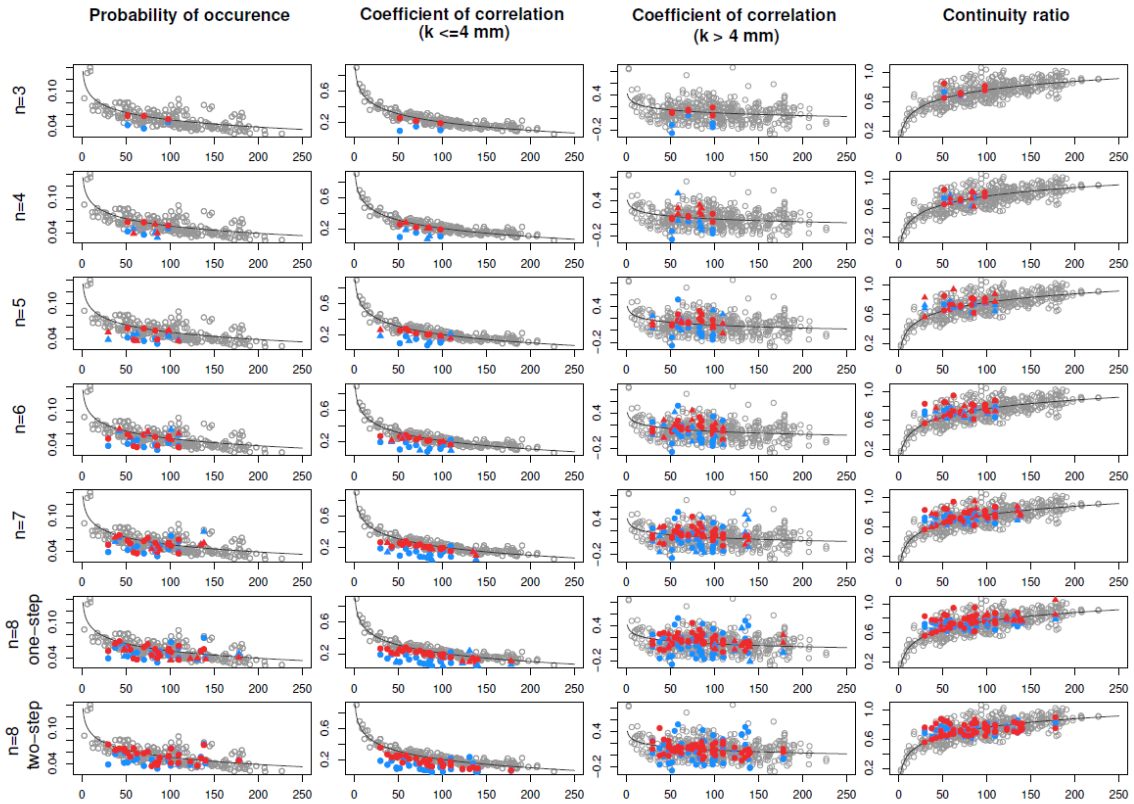

518

519 Fig. 8. Rainfall characteristics before (blue) and after (red) resampling of disaggregated time series using the
520 one-step approach (line 1 – 6) and the two-step approach (line 7). The number of involved stations is increased
521 by one in line 1 - 6. The added station in the one-step approach is marked by triangles, previously considered
522 stations by circles. The grey circles represent the empirical values of the investigation area. For the two-step-
523 approach no differentiation is done. Additionally, the corresponding regression line is included.

524

525 The values for the continuity ratio are within the cloud of observed values after the
526 disaggregation and remain there after applying both resampling approaches. Omitting this
527 characteristic from the objective function was also tested. Results showed that continuity ratio
528 values worsened and moved outside of the observation cloud. Therefore this characteristic
529 remained included. However, after the resampling, the values of the continuity ratio cover a
530 wider range than before the resampling for each distance. This may be caused by the
531 definition of the criterion, taking only station *k* with respect to station *l* into account, but not
532 vice versa. However the continuity ratio of station *l* with respect to station *k* is different, since

other time steps are taken into account. Hence, continuity ratio $C_{k,l}$ can be improved by simultaneous worsening of $C_{l,k}$.

The probability of occurrence is lower than for observed time series after the disaggregation. With resampling of three stations, the probability values could be adjusted closer to the observed ones. If more than three stations are included in the resampling of the one-step approach, some of the probability values cannot be shifted closer to the observed values, while for the two-step approach almost all probabilities are within the cloud of observations. The advantage of the two-step approach with a smaller number of reference stations in the second step, is that it causes a higher degree of freedom and a better fit seems possible.

For the coefficient of correlation ($k > 4$ mm), almost all values of the disaggregated time series are already within the observation cloud before applying the resampling algorithm. However after the resampling, all coefficients are within the observation cloud. Omitting this characteristic from the objective function was also investigated. Without this criterion, extremes of areal rainfall were overestimated (not shown here). Hence this rainfall characteristic was not omitted from the objective function.

The coefficient of correlation ($k \leq 4$ mm) is underestimated by the disaggregated time series. For all stations, the coefficients were shifted closer to the observed values by the resampling procedure. Using three stations leads to values comparable to the observations for the coefficient of correlation ($k \leq 4$ mm). For eight stations, there are some values still below the observations for the one-step approach. This underestimation is not related to distance. For the two-step approach a higher number of underestimations can be identified. Since the two-step approach has shown improvement for the probability of occurrence, the underestimation must be caused by the missing information of rainfall amount of stations from *U1* and *U1-others* during the resampling process.

For further investigation, the areal rainfall of the Aller-Leine river basin and the Upper-Leine subcatchment were analyzed: The non-exceedance curves of areal rainfall intensities ≥ 0.1 mm, for both the diversion and the uniform splitting method and before and after the annealing, are shown in Fig. 9 for the Upper Leine subcatchment and in Fig. 10 for the Aller-Leine river basin (see Fig. 5 for an overview of the data sets). The shape of the non-exceedance curves, taking into account lower rainfall intensities, show only small variations below 0.1 mm and are not illustrated here.

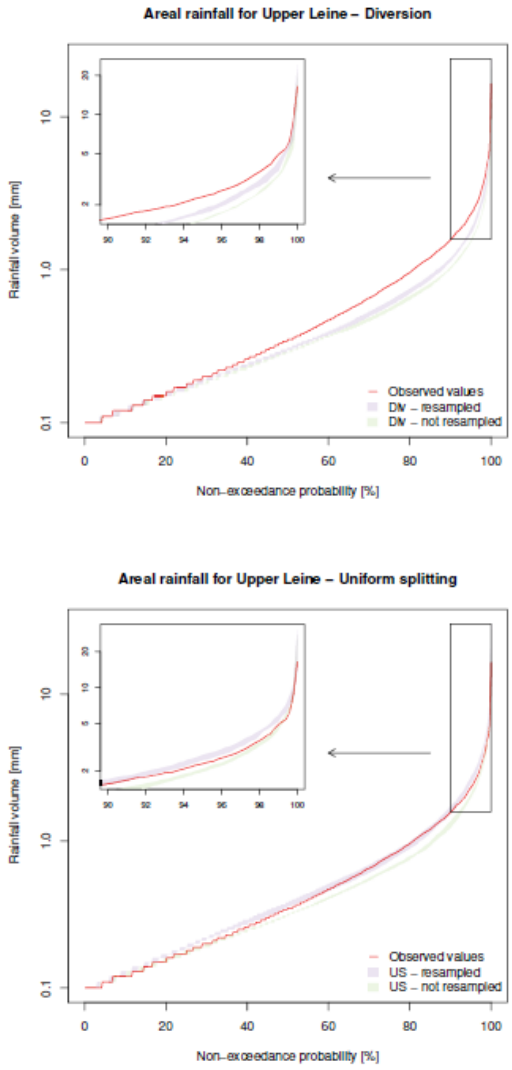

Fig. 9. Non-exceedance curves of all areal rainfall intensities ≥ 0.1 mm for the Upper Leine catchment for observed and disaggregated time series before and after using simulated annealing – for a) diversion (Div) and b) uniform splitting (US). The shaded areas represent the enveloping curves of all 9 realizations for each method.

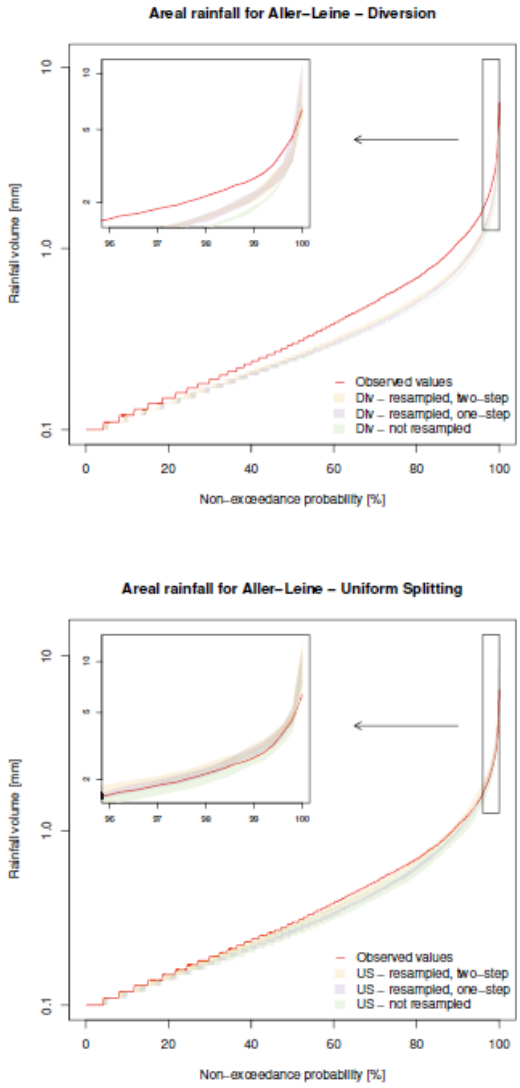

568

569 Fig. 10. Non-exceedance curves of all areal rainfall intensities ≥ 0.1 mm for the Aller-Leine river basin for
570 observed and disaggregated time series before and after using simulated annealing – for a) diversion (Div) and b)
571 uniform splitting (US). The shaded areas represent the enveloping curves of the data sets used for each method.

572

573 Using the diversion method for disaggregation of rainfall without the subsequent annealing
574 procedure leads to an underestimation of areal rainfall for the whole rainfall volume spectrum.
575 After resampling, the non-exceedance curve is closer to the one from the observations for
576 non-exceedance probabilities higher than 20 %. For smaller values, only slight changes can be
577 found after the resampling.

578 Uniform splitting also results in a non-exceedance curve which underestimates the
579 observations for non-exceedance probabilities greater than 30 %. However, these
580 underestimations are smaller than in comparison to the diversion method. After the
581 application of the annealing algorithm, observed areal rainfall from 60 % (representing
582 0.4 mm) up to 90 % (1.3 mm) is within the range of the simulated realisations. For other non-
583 exceedance probabilities, areal rainfall is slightly overestimated after the resampling.

584 For the Aller-Leine river basin, the diversion leads to an underestimation of rainfall volume,
585 again for the whole spectrum (except for the highest values). The non-exceedance curve is
586 underestimated, regardless of whether the resampling algorithm is applied or not. It should be
587 mentioned that when taking into account areal rainfall intensities smaller than 0.1 mm, non-
588 exceedance probabilities are overestimated (not shown here). This is contradictory to the
589 underestimation of areal rainfall that was estimated without implementing spatial consistence.
590 The reason for this contrast is the overestimated fraction in the time series of wet intervals of
591 very small intensity generated by the diversion. With an increasing number of stations, the
592 probability of small rainfall events occurring simultaneously also increases.

593 For the uniform splitting, a better visual fit is achieved for all data sets than for the diversion.
594 All three data sets have similar curves of non-exceedance probability below approximately
595 20 %. For non-exceedance probabilities in the range between 20 % (about 0.15 mm) and 90 %
596 (1.1 mm), the two-step approach shows the best fit to the observed areal rainfalls. For rainfall
597 intensities greater than 1.5 mm (~95 % non-exceedance probability), the ranges of all three
598 data sets unify to an identical curve.

599

600

601

Summary and Conclusions

In this study two novelties were presented. First, a modified multiplicative random cascade model (called uniform splitting) is introduced, which is parameter parsimonious and able to disaggregate daily rainfall values to hourly values. Modifications to this model are the application of a branching number $b = 3$ in the first disaggregation step similar to Lisniak et al. (2013) and the introduction of an upper quantile class for daily rainfall amounts ($>q_{0.998}$). The performance of the model was compared with observed values from the Aller-Leine catchment in Lower Saxony (Germany) and another modified cascade model, introduced by Güntner et al. (2001). Different criteria regarding time series statistics, the non-exceedance curve of the rainfall intensities and extreme values were taken into account for the evaluation. The following conclusions can be drawn:

1. The uniform splitting provides better results than the diversion for basic event characteristics and the non-exceedance curve of rainfall intensities.
2. The statistics of the observed time series could be reproduced well by the uniform splitting. Slight underestimations of fraction of dry intervals, wet and dry spell duration (3 %, 12 % and 6 %) and an overestimation of the average rainfall intensity (4 %), can be identified.
3. The non-exceedance curve of the rainfall intensities generated by the uniform splitting shows a good visual fit between 35 % and 93 %. Rainfall for higher non-exceedance probabilities is slightly overestimated.
4. Observed extreme values can be reproduced reasonably well by the uniform splitting. All observed values are enveloped by the range of all 80 disaggregation runs. The median shows slight overestimations for some stations.

For all disaggregated time series, one third of all rainfall intensities are smaller than the lowest observed rainfall intensity. This conforms to Molnar & Burlando (2005), who found a similar problem, with 48 % of all wet values smaller than the measuring accuracy.

It should be mentioned, that the autocorrelation of the time series cannot be reproduced by the micro-canonical cascade model (Lombardo et al., 2012). This remains a problem that has not been solved yet for random cascades to the authors' knowledge. However, with the main interest in the representation of event characteristics and duration curves, this disadvantage was taken into account (see also the discussion in Lisniak et al., 2013).

The second novelty of this study is the implementation of spatial consistence subsequent to the disaggregation procedure. The essential findings are:

5. All bivariate characteristics could be improved by the annealing algorithm.
6. The resampling improved all non-exceedance curves of areal rainfall, independent of the chosen disaggregation method and the catchment. The annealing algorithm reduces over- and underestimations.
7. Time series based on the uniform splitting show a higher capability to implement spatial consistence than the time series based on the diversion.

For the resampling, a one-step and a two-step approach were investigated in the Aller-Leine river basin. The resulting conclusions are:

8. The number of stations limits a good reproduction for probability of occurrence in the one-step and for the coefficient of correlation ($k \leq 4$ mm) in the two-step approach.
9. The two-step approach yields a slightly better representation of the non-exceedance curve than the one-step approach.

It should be mentioned that the introduced uniform splitting uses unbounded, scale-independent parameters. However, the overall performance of the uniform splitting was better

649 in comparison to the diversion for the investigated time series. Thus, it should be applied to
650 different climate regions to test its transferability and to prove if this statement holds.

651 The annealing algorithm shows potential to improve spatial characteristics and hence for
652 implementing spatial consistence. Next steps for a better representation of spatial rainfall
653 could be the investigation of additional objective criteria like e.g. the log-odd ratio (Mehrotra
654 et al., 2006) in the objective function or the introduction of multivariate criteria beside the
655 bivariate ones. Further investigations should also be done for smaller catchments, since the
656 temporal connection of rainfall occurrence and intensity is important in view of rainfall-
657 runoff-modeling and other applications. An adaption of the simulated annealing for other
658 disaggregation models seems possible with little change in the algorithm concerning the
659 structure of the time series which should be preserved. For a multivariate resampling the
660 annealing algorithm can be modified, e.g. for each resampling of relative diurnal cycles two
661 stations are drawn randomly beforehand. This simultaneous resampling would increase the
662 degrees of freedom in comparison to the sequential resampling.

663 Generally, it seems possible to generate high-resolution time series with spatial consistence of
664 either observed daily values or climate projected rainfall data for different applications
665 through use of the uniform splitting method in combination with the subsequent annealing
666 algorithm.

667

668 **Acknowledgements**

669 The authors thank Jennifer Ullrich for calibration of the simulated annealing parameters and
670 Christian Berndt and Ross Pidoto for useful comments on an early draft of the manuscript.
671 We are also thankful for the permission to use the data of the German National Weather

672 Service (Deutscher Wetterdienst DWD) and Meteomedia AG. Finally, the two reviewers and
673 the editor are gratefully acknowledged for their contributions to improve this publication.

674

675 **References**

676 Aarts, E., Korst, J. (1965). "Simulated Annealing and Boltzmann Machines: A stochastic
677 approach to combinatorial optimization and neural computing." John Wiley & Sons,
678 Chichester.

679 Bardossy, A. (1998). "Generating precipitation time series using simulated annealing." *Water*
680 *Resour. Res.*, 34(7), 1737-1744, 1998.

681 Breinl, K., Turkington, T., Stowasser, M. (2013). "Stochastic generation of multi-site daily
682 precipitation for applications in risk management." *J. Hydrol.*, 498(0), 23-35

683 Breinl, K., Turkington, T., Stowasser, M. (2014). "Simulating daily precipitation and
684 temperature: a weather generation framework for assessing hydrometeorological hazards."
685 *Meteorol. Appl.*, in press.

686 Buishand, T. A. (1977). "Stochastic modeling of daily rainfall sequences." H. Veenmann &
687 Zonen B. V., Wageningen.

688 Carsteanu, A., Foufoula-Georgiou, E. (1996). "Assessing dependence among weights in a
689 multiplicative cascade model of temporal rainfall." *J. Geophys. Res.*, 101(D21), 26363-26370.

690 Goovaerts, P. (2000). "Geostatistical approaches for incorporating elevation into spatial
691 interpolation of rainfall." *J. Hydrol.*, 228(1-2), 113-129.

692 Güntner, A., Olsson, J., Calver, A., Gannon, B. (2001). "Cascade-based disaggregation of
693 continuous rainfall time series: the influence of climate." *Hydrol. Earth Syst. Sc.*, 5(2), 145-
694 164.

695 Gupta, V. J., Waymire, E. C. (1993). “A statistical analysis of mesoscale rainfall as a random
696 cascade.” *J. Appl. Meteorol.*, 32(2), 251-267.

697 Haberlandt, U., Ebner von Eschenbach, A. D., Buchwald, I. (2008). „A space-time hybrid
698 hourly rainfall model for derived flood frequency analysis.” *Hydrol. Earth Syst. Sc.*, 12(6),
699 1353-1367.

700 Jebari, S., Berndtsson, R., Olsson, J., Bahri, A. (2012). “Soil erosion estimation based on
701 rainfall disaggregation.” *J. Hydrol.*, 436-437(0), 102-110.

702 Kirkpatrick, S., Gelatt, C. D., Vecchi, M. P. (1983). „Optimization by simulated annealing.”
703 *Science*, 220(4598), 671-680.

704 Koutsoyiannis, D., Onof, C., Wheater, H. S. (2003). “Multivariate rainfall disaggregation at a
705 fine time scale.” *Water Resour. Res.*, 39(7), 1173.

706 Koutsoyiannis, D., Langousis, A. (2011). “Precipitation.” *Treatise on water science*, P.
707 Wilderer and S. Uhlenbrook, eds., volume 2, Oxford: Academic Press, 27-78.

708 Mehrotra, R., Srikanthan, R., Sharma, A. (2006). “A comparison of three stochastic multi-site
709 precipitation occurrence generators.” *J. Hydrol.*, 331(1-2), 280-292.

710 Licznar, P., Lomotowski, J., Rupp, D. E. (2011). “Random cascade driven rainfall
711 disaggregation for urban hydrology: An evaluation six models and a new generator.” *Atmos.*
712 *Res.*, 99(3-4), 563-578.

713 Lisniak, D., Franke, J., Bernhofer, C. (2013). “Circulation pattern based parameterization of a
714 multiplicative random cascade for disaggregation of observed and projected daily rainfall time
715 series.” *Hydrol. Earth Syst. Sc.*, 17(7), 2487-2500.

716 Lombardo, F., Volpi, E., Koutsoyiannis, D. (2012). “Rainfall downscaling in time: theoretical
717 and empirical comparison between multifractal and Hurst-Kolmogorv discrete random
718 cascades.” *Hydrolog. Sci. J.*, 57(6), 1052-1066.

719 Mandelbrot, B. (1974): “Intermittent turbulence in self-similar cascades – divergence of high
720 moments and dimension of carrier.” *J. Fluid Mech.*, 62(2), 331-358.

721 Marshak, A., Davis, A., Cahalan, R., Wiscombe, W. (1994). “Bounded cascade models as
722 nonstationary multifractals.” *Phys. Rev. E*, 49(1), 55-69.

723 Molnar, P., Burlando, P. (2005). “Preservation of rainfall properties in stochastic
724 disaggregation by a simple random cascade model.” *Atmos. Res.*, 77(1-4), 137-151.

725 Olsson, J. (1998). “Evaluation of a scaling cascade model for temporal rainfall
726 disaggregation.” *Hydrol. Earth Syst. Sc.*, 2(1), 19-30.

727 Peel, M. C., Finlayson, B.L., McMahon, T. A. (2007). “Updated world map of the Köppen-
728 Geiger climate classification.” *Hydrol. Earth Syst. Sc.*, 11(5), 1633-1644.

729 Rupp, D. E., Keim, R. F., Ossiander, M., Brugnach, M., Selker, J. (2009). „Time scale and
730 intensity dependency in multiplicative cascades for temporal rainfall disaggregation.” *Water*
731 *Resour. Res.*, 45(7), W07409.

732 Schertzer, D., Lovejoy, S. (1987). “Physical Modeling and analysis of rain and clouds by
733 anisotropic scaling multiplicative processes.” *J. Geophys. Res.*, 92(D8), 9693-9714.

734 Veneziano, D., Furcolo, P., Iacobellis, V. (2006). “Imperfect scaling of time and space-time
735 rainfall.” *J. Hydrol.*, 322(1-4), 105-119.

736 Weibull, W. (1939). “The Phenomen of Rupture in Solids.” Ingeniors Vetenskaps Akadamien
737 Handlinge 153, Stockholm, p. 17

738 Wilks, D. S. (1998). “Multisite generalization of a daily stochastic precipitation generation
739 model.” *J. Hydrol.*, 210(1-4), 178-191.